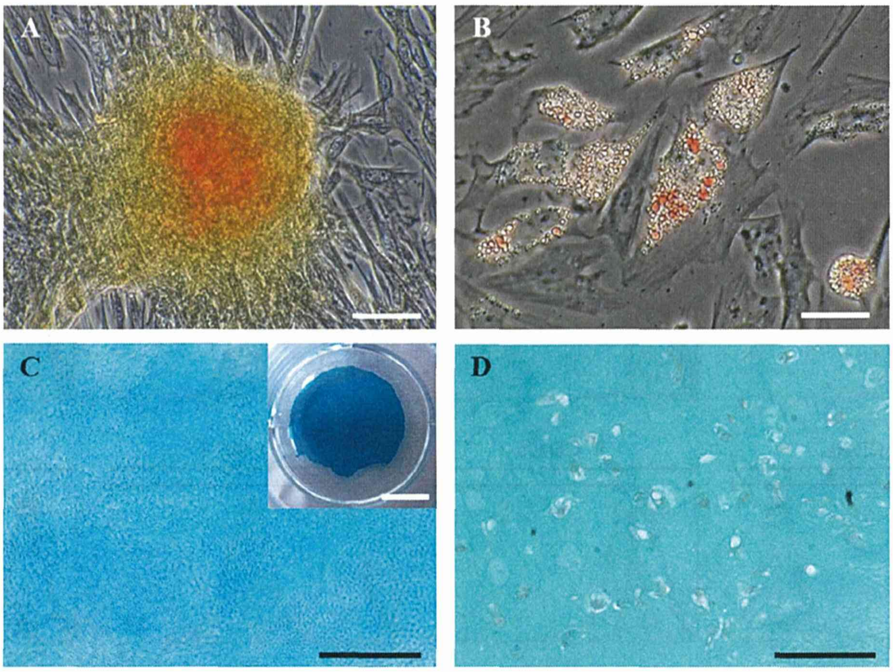

Fig. 5. Representative images showing staining with alizarin red for osteogenic differentiation (A), oil red O for adipogenic differentiation (B) and Alcian blue for chondrogenic differentiation (C and D) of synovial fluid (SF)-derived mesenchymal stem cells (MSCs). Following 2 weeks of osteogenic induction, the SF-MSCs aggregated and contracted to form colonies, and produced a specific matrix including calcium apatite crystals, which were positively stained with alizarin red. Scale bar = 100 µm (A). Adipogenic induction of SF-MSCs resulted in adipocyte-like flattened cells with small lipid vesicles that stained red with oil red O. Scale bar = 50 µm (A). Plate culture of SF-MSCs in chondrogenic induction medium induced a change in cell shape into a 'stone-wall' structure. Scale bar = 500 µm. A gelatinous monolayer sheet was present that intensely stained with Alcian blue. Scale bar = 1 cm in the inset picture (C). Histological preparation of cell pellets showing a hyaline cartilage-like structure that was positively stained with Alcian blue. Scale bar = 100 µm (D).

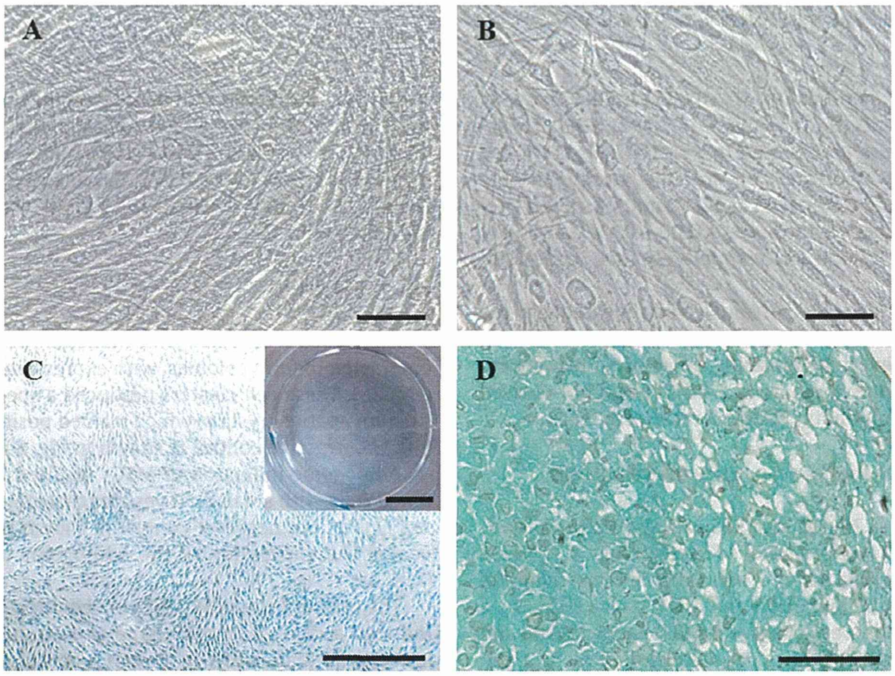

Fig. 6. Representative images showing synovial fluid (SF)-derived mesenchymal stem cells (MSCs) stained with alizarin red (A), oil red O (B) and Alcian blue (C and D). The negative controls were cultured with complete culture medium (CCM) during the corresponding periods of time taken to induce osteogenic, adipogenic and chondrogenic differentiation (A–C). The negative control for the cell pellet (D) was cultured in chondrogenic induction medium without transforming growth factor (TGF)-β3. Positive staining was not seen in (A) or (B) and no gelatinous monolayer sheet was formed (D). Chondrocyte and hyaline matrices were not seen in the pellet (D).

Please cite this article in press as: D. Murata, et al., Multipotency of equine mesenchymal stem cells derived from synovial fluid, The Veterinary Journal (2014), doi: 10.1016/j.tvjl.2014.07.029

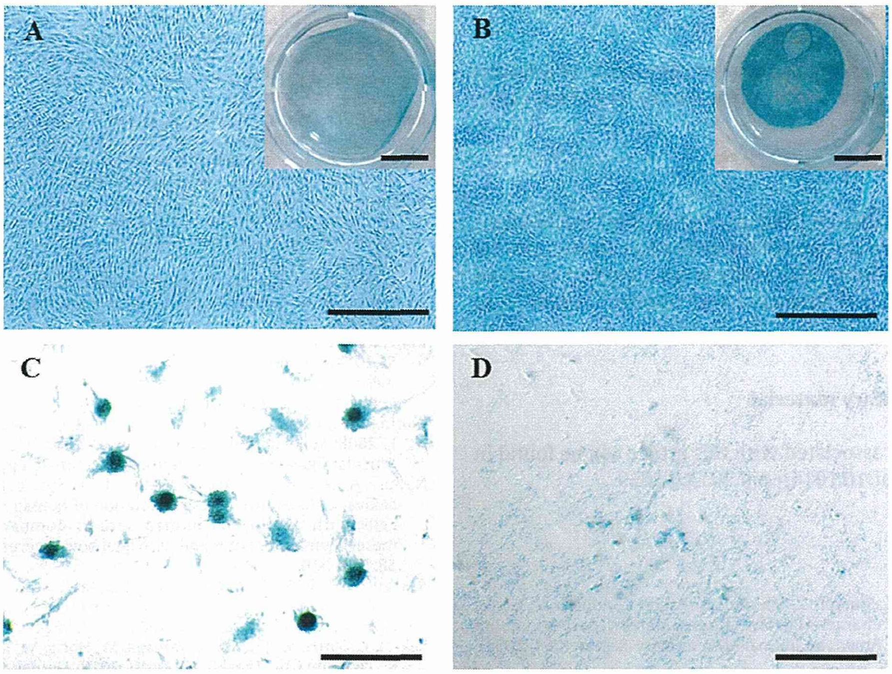

Fig. 7. Representative images showing Alcian blue staining of plate cultures of synovial fluid (SF)-derived mesenchymal stem cells (MSCs), adipose tissue (AT)-derived MSCs and bone marrow (BM)-derived MSCs after chondrogenic induction. Staining of the gelatinous sheets in SF-MSCs was intensely blue at passage 10 (P10) from the diseased joints (A), as well as SF-MSCs from the normal joints (B). Blue sheets were not formed following chondrogenic induction of AT-MSCs and BM-MSCs (C and D). Scale bar = 500 µm.

following chondrogenic induction (Figs. 7c and d). RT-PCR revealed elevated expression of marker genes specific for chondrogenesis, including Sox-9, Col-II and aggrecan (Fig. 2d). Histological observation of the cell pellets showed a hyaline cartilage-like structure that was positively stained with Alcian blue (Fig. 5d, negative control is shown in Fig. 6d) and which abundantly expressed cartilage-specific molecules, such as COMP in the extracellular matrix (see Appendix: Supplementary Fig. S4). RT-PCR revealed the expression of tenogenic marker genes, such as Scx and TenC (Fig. 2e).

Discussion

In the present study, equine SF from joints with osteochondral fragments included spindle-shaped cells that adhered to culture dishes and proliferated to form colonies; these findings correspond to the distinctive features of human MSCs (Friedenstein, 1976). Previously defined markers for MSCs, in which CD44, CD90 and CD105, but not CD34 or CD45, are expressed (Morito et al., 2008; Sekiya et al., 2012), were identical in the cells derived from equine SF, as well as equine AT-MSCs and BM-MSCs, in the present study. In addition to these results, the ability of these cells to differentiate into osteoblasts, chondrocytes, adipocytes and tenocytes was also a feature of equine SF-MSCs, as well as equine AT-MSCs and BM-MSCs. If we can efficiently and effectively isolate and increase the number of cells, SF could be a useful source of equine MSCs for equine cartilage regeneration, since arthrocentesis to collect SF is less invasive and has a lower risk of contamination with infectious agents compared to collection of BM or AT.

In this study, we used SF from injured joints, which produced small numbers of colonies of MSCs at P0 and reached a total number of $>1 \times 10^5$ cells at P1. In a human study, MSCs were detected at very low densities in SF from normal volunteers, but increased with the grade of osteoarthritis (Sekiya et al., 2012). In the present study, we showed that the number of colonies of SF-MSCs at P0 was significantly increased in equine SF from diseased joints compared to normal joints. Since fewer MSCs are present in normal SF, the increased numbers of the cells in SF from diseased or injured joints suggest that SF-MSCs could play a role in the process of degradation, repair and regeneration of damaged cartilage. On the basis of morphology and gene profile, SF-MSCs were more similar to synovium-derived MSCs than to BM-MSCs (Sekiya et al., 2012). Another study suggested that human SF-MSCs are released from the synovium in association with joint insults (Nimura et al., 2008); we speculate that equine SF-MSCs may be released from the synovium, especially in cases of OCD.

In our study, plate culture of SF-MSCs from normal or diseased joints in chondrogenic induction medium induced a change in the cell shape to a 'stone-wall' structure typical of chondrogenic differentiation, followed by formation of a gelatinous monolayer that was intensely stained with Alcian blue. However, chondrogenic induction of AT-MSCs and BM-MSCs resulted in no blue gelatinous sheet. A previous report suggested that SF-MSCs may be a superior source of cells for autologous transplantation for cartilage regeneration in human beings (Sakaguchi et al., 2005). Our results suggest that equine SF might be a superior source of MSCs for cartilage regeneration, but more definitive results would be needed to conclude that SF-MSCs could be suitable for generating cartilage matrix during chondrogenic differentiation compared to AT-MSCs or BM-MSCs.

Conclusions

Equine SF may be a novel source of multipotent MSCs that have the ability to regenerate chondrocytes. Since collecting SF is less invasive than collecting BM or AT, SF-MSCs could be used to develop a practical strategy for cartilage regeneration following arthroscopic surgery in horses.

Please cite this article in press as: D. Murata, et al., Multipotency of equine mesenchymal stem cells derived from synovial fluid, The Veterinary Journal (2014), doi: 10.1016/j.tvjl.2014.07.029

Conflict of interest statement

None of the authors has any financial or personal relationships that could inappropriately influence or bias the content of the paper.

Acknowledgements

The authors acknowledge Dr Douglas Antczak, Mr Donald Miller and Ms Becky Harman for the gifts of the antibodies against CD11a/18, and MHC classes I and II. This study was supported by Japan Society for the Promotion of Science (Grant number 25660242 to KM).

Appendix: Supplementary material

Supplementary data associated with this article can be found in the online version at doi:10.1016/j.tvjl.2014.07.029.

References

Arnhold, S.J., Goletz, I., Klein, H., Stumpf, G., Beluche, L.A., Rohde, C., Addicks, K., Litzke, L.F., 2007. Isolation and characterization of bone marrow-derived equine mesenchymal stem cells. American Journal of Veterinary Research 68, 1095–1105.

Barberini, D.J., Freitas, N.P., Magnoni, M.S., Maia, L., Listoni, A.J., Heckler, M.C., Sudano, M.J., Golim, M.A., Landim-Alvarenga, F.D., Amorim, R.M., 2014. Equine mesenchymal stem cells from bone marrow, adipose tissue and umbilical cord: Immunophenotypic characterization and differentiation potential. Stem Cell Research and Therapy 5, 25.

Braun, J., Hack, A., Weis-Klemm, M., Conrad, S., Treml, S., Kohler, K., Walliser, U., Skutella, T., Aicher, W.K., 2010. Evaluation of the osteogenic and chondrogenic differentiation capacities of equine adipose tissue-derived mesenchymal stem cells. American Journal of Veterinary Research 71, 1228–1236.

Burk, J., Ribitsch, I., Gittel, C., Juelke, H., Kasper, C., Staszyk, C., Brehm, W., 2013. Growth and differentiation characteristics of equine mesenchymal stromal cells derived from different sources. The Veterinary Journal 195, 98–106.

Friedenstein, A.J., 1976. Precursor cells of mechanocytes. International Review of Cytology 47, 327–359.

Jones, E.A., English, A., Henshaw, K., Kinsey, S.E., Markham, A.F., Emery, P., McGonagle, D., 2004. Enumeration and phenotypic characterization of synovial fluid multipotential mesenchymal progenitor cells in inflammatory and degenerative arthritis. Arthritis and Rheumatism 50, 817–827.

Kearns, C.F., McKeever, K.H., Malinowski, K., Struck, M.B., Abe, T., 2001. Chronic administration of therapeutic levels of clenbuterol acts as a repartitioning agent. Journal of Applied Physiology 91, 2064–2070.

Lee, J.I., Sato, M., Kim, H.W., Mochida, J., 2011. Transplantation of scaffold-free spheroids composed of synovium-derived cells and chondrocytes for the treatment of cartilage defects of the knee. European Cells and Materials 22, 275–290.

Mohanty, N., Gulati, B.R., Kumar, R., Gera, S., Kumar, P., Somasundaram, R.K., Kumar, S., 2014. Immunophenotypic characterization and tenogenic differentiation of mesenchymal stromal cells isolated from equine umbilical cord blood. In Vitro Cellular and Developmental Biology. Animal 50, 538–548.

Morito, T., Muneta, T., Hara, K., Ju, Y.J., Mochizuki, T., Makino, H., Umezawa, A., Sekiya, I., 2008. Synovial fluid-derived mesenchymal stem cells increase after intra-articular ligament injury in humans. Rheumatology 47, 1137–1143.

Nimura, A., Muneta, T., Koga, H., Mochizuki, T., Suzuki, K., Makino, H., Umezawa, A., Sekiya, I., 2008. Increased proliferation of human synovial mesenchymal stem cells with autologous human serum: Comparisons with bone marrow mesenchymal stem cells and with fetal bovine serum. Arthritis and Rheumatism 58, 501–510.

Sakaguchi, Y., Sekiya, I., Yagishita, K., Muneta, T., 2005. Comparison of human stem cells derived from various mesenchymal tissues: Superiority of synovium as a cell source. Arthritis and Rheumatism 52, 2521–2529.

Sekiya, I., Ojima, M., Suzuki, S., Yamaga, M., Horie, M., Koga, H., Tsuji, K., Miyaguchi, K., Ogishima, S., Tanaka, H., et al., 2012. Human mesenchymal stem cells in synovial fluid increase in the knee with degenerated cartilage and osteoarthritis. Journal of Orthopaedic Research 30, 943–949.

Suzuki, S., Muneta, T., Tsuji, K., Ichinose, S., Makino, H., Umezawa, A., Sekiya, I., 2012. Properties and usefulness of aggregates of synovial mesenchymal stem cells as a source for cartilage regeneration. Arthritis Research and Therapy 14, R136.

Vidal, M.A., Kilroy, G.E., Lopez, M.J., Johnson, J.R., Moore, R.M., Gimble, J.M., 2007. Characterization of equine adipose tissue-derived stromal cells: Adipogenic and osteogenic capacity and comparison with bone marrow-derived mesenchymal stromal cells. Veterinary Surgery 36, 613–622.

Dear Author,

Here are the final proofs of your article. Please check the proofs carefully.

All communications with regard to the proof should be sent to bmcproductionteam2@spi-global.com.

Please note that at this stage you should only be checking for errors introduced during the production process. Please pay particular attention to the following when checking the proof:

- Author names. Check that each author name is spelled correctly, and that names appear in the correct order of first name followed by family name. This will ensure that the names will be indexed correctly (for example if the author's name is 'Jane Patel', she will be cited as 'Patel, J.').
- Affiliations. Check that all authors are cited with the correct affiliations, that the author who will receive correspondence has been identified with an asterisk (*), and that all equal contributors have been identified with a dagger sign (†).
- Ensure that the main text is complete.
- Check that figures, tables and their legends are included and in the correct order.
- Look to see that queries that were raised during copy-editing or typesetting have been resolved.
- Confirm that all web links are correct and working.
- Ensure that special characters and equations are displaying correctly.
- Check that additional or supplementary files can be opened and are correct.

Changes in scientific content cannot be made at this stage unless the request has already been approved. This includes changes to title or authorship, new results, or corrected values.

How to return your corrections

Returning your corrections via online submission:
- Please provide details of your corrections in the online correction form. Always indicate the line number to which the correction refers.

Returning your corrections via email:
- Annotate the proof PDF with your corrections.
- Send it as an email attachment to: bmcproductionteam2@spi-global.com.
- Remember to include the journal title, manuscript number, and your name when sending your response via email.

After you have submitted your corrections, you will receive email notification from our production team that your article has been published in the final version. All changes at this stage are final. We will not be able to make any further changes after publication.

Kind regards,

BioMed Central Production Team 2

Murata et al. Journal of Orthopaedic Surgery and Research _####################_
DOI 10.1186/s13018-015-0173-0

JOURNAL OF ORTHOPAEDIC SURGERY AND RESEARCH

RESEARCH ARTICLE Open Access

A preliminary study of osteochondral regeneration using a scaffold-free three-dimensional construct of porcine adipose tissue-derived mesenchymal stem cells

Daiki Murata[1], Satoshi Tokunaga[2], Tadashi Tamura[3], Hiroaki Kawaguchi[4], Noriaki Miyoshi[4], Makoto Fujiki[1], Koichi Nakayama[5] and Kazuhiro Misumi[1*]

Abstract

Background: Osteoarthritis (OA) is a major joint disease in humans and many other animals. Consequently, medical countermeasures for OA have been investigated diligently. This study was designed to examine the regeneration of articular cartilage and subchondral bone using three-dimensional (3D) constructs of adipose tissue-derived mesenchymal stem cells (AT-MSCs).

Methods: AT-MSCs were isolated and expanded until required for genetical and immunological analysis and construct creation. A construct consisting of about 760 spheroids that each contained 5.0×10^4 autologous AT-MSCs was implanted into an osteochondral defect (diameter: 4 mm; depth: 6 mm) created in the femoral trochlear groove of two adult microminipigs. After implantation, the defects were monitored by computed tomography every month for 6 months in animal no. 1 and 12 months in animal no. 2.

Results: AT-MSCs were confirmed to express the premature genes and to be positive for CD90 and CD105 and negative for CD34 and CD45. Under specific nutrient conditions, the AT-MSCs differentiated into osteogenic, chondrogenic, and adipogenic lineages, as evidenced by the expressions of related marker genes and the production of appropriate matrix molecules. A radiopaque area emerged from the boundary between the bone and the implant and increased more steadily upward and inward for the implants in both animal no. 1 and animal no. 2. The histopathology of the implants after 6 months revealed active endochondral ossification underneath the plump fibrocartilage in animal no. 1. The histopathology after 12 months in animal no. 2 showed not only that the diminishing fibrocartilage was as thick as the surrounding normal cartilage but also that massive subchondral bone was present.

Conclusions: The present results suggest that implantation of a scaffold-free 3D construct of AT-MSCs into an osteochondral defect may induce regeneration of the original structure of the cartilage and subchondral bone over the course of 1 year, although more experimental cases are needed.

Keywords: Regeneration, Cartilage, Bone, Scaffold-free, Three-dimensional construct, Stem cell, Adipose tissue, Computed tomography, Histopathology, Porcine

* Correspondence: kaz_msm@vet.kagoshima-u.ac.jp
[1]Veterinary Surgery, Department of Veterinary Clinical Science, Joint Faculty of Veterinary Medicine, Kagoshima University, 21-24 Korimoto 1-chome, Kagoshima 890-0065, Japan
Full list of author information is available at the end of the article

Background

Osteoarthritis (OA) is a major joint disease contributing to midlife and geriatric locomotor dysfunction, and the associated disability can decrease quality of life in humans [1]. OA slowly progresses not only as a result of traumatic injuries to joint structures [2] but also through many exacerbating factors such as age, sex, body mass index, occupation, bone shape, and genetic factors regulating proteolytic enzymes [3-5]. In advanced OA, cartilage degeneration and subchondral bone sclerosis may be worsened by the usual mechanical load of daily activities [6], and therefore surgical strategies to reconstruct both the bone and cartilage have been investigated to restore joint structure and function [7]. A particular issue of interest in recent studies has been the complete regeneration of hyaline cartilage covering the subchondral bone.

Although a clinical study of osteochondral autografts from non-load-bearing sites implanted into deteriorated sites showed favorable outcomes following surgery (clinical improvement in 79%–94% of OA patients) [8], a loss of clinically sound cartilage at the donor sites is associated with autologous osteochondral transfer [9]. Studies on surgical procedures using a combination of artificial bone and autologous chondrocytes seeded into a collagen scaffold have also shown favorable restoration of cartilage [10,11]. However, some studies have suggested associated problems such as isolation of few chondrocytes from a small piece of normal cartilage [10] and dedifferentiation of chondrocytes during passages in culture [12]. To solve these problems, stem cells have recently received attention in a study [13].

Stem cells are defined as immature cells that have the ability for self-renewal and the potential for multilineage differentiation into specific cells. Mesenchymal stem cells (MSCs) derived from bone marrow (BM) and adipose tissue (AT) have mostly been used to demonstrate differentiation into bone and cartilage in vitro [14,15]. BM-derived MSCs (BM-MSCs) appear to have some disadvantages including decreased numbers and deterioration of the cells depending on senescence and natural transformation caused by genomic instability [16]. Previous experiments have shown age-related decreases in the yield rate, growth rate, and differentiation potential of BM-MSCs in rats and humans [17,18]. On the other hand, the advantages of AT-derived MSCs (AT-MSCs) are that abundant cells can be isolated from AT and their cellular proliferation rate may be higher in mature animals [19]. Furthermore, given that obesity is undesirable in OA patients, the regenerative strategy for bone and cartilage using unwanted AT could be reasonable and acceptable by many OA patients. It has been reported that AT-MSCs hardly differentiate into chondrocytes [20]. However, a recent study using rabbits demonstrated the regeneration of bone and cartilage after implantation of scaffold-free three-dimensional (3D) constructs of AT-MSCs into osteochondral defects [21]. This report also contains a novel strategy for scaffold-free cell implantation.

Previous studies indicated that scaffolds composed of materials such as collagen and hyaluronic acid could be useful for promoting cell adhesion, proliferation, and chondrogenic differentiation [22,23], and bone regeneration using AT-MSCs seeded into hydroxyapatite has also been investigated [24]. However, artificial materials may induce xenobiotic reactions through immune reactions in the tissue [25].

In many previous studies, bone and cartilage regeneration through various cell therapies has been evaluated in the knee joint of rabbits [26-30]. However, to obtain meaningful results that are appropriate for extrapolating bone and cartilage regeneration to human OA, we expect that pigs will provide a more appropriate animal model than rabbits. Microminipigs (MMPigs) have similar behavior patterns to human daily life, as they spend time standing and walking in the daytime and sleeping at night [31,32]. In contrast, rabbits usually sit in cages. This study was designed to evaluate the regeneration of articular cartilage and subchondral bone using 3D constructs of autologous AT-MSCs in MMPigs.

Materials and methods

Animals

Two MMPigs (Fuji Micra, Shizuoka, Japan), designated animal no. 1 (male) and animal no. 2 (female), were used in this study. Their body weights and ages were 13.8 kg and 25 months, and 14.6 kg and 23 months, respectively. All procedures in this study were approved by the Animal Care and Use Committee of Kagoshima University (Approval No. A11037). Ten to fifteen grams of cervical AT per animal was aseptically obtained under general anesthesia.

Isolation and expansion of AT-MSCs

The AT samples were minced and digested for 90 min in phosphate-buffered saline (PBS) containing 0.1% collagenase (Collagenase Type I; Worthington Biochemical, Lakewood, NJ). The digested cell suspensions were filtered through a 70-μm-pore-diameter membrane (Cell Strainer; BD, Franklin Lakes, NJ) and centrifuged at $160 \times g$ for 5 min at room temperature. After decanting the supernatant, the pellet was resuspended with PBS and centrifuged. The supernatant was removed, and the pellet was resuspended and plated on a 150-cm^2 culture dish (Tissue Culture Dish ϕ 150; TPP, Trasadingen, Switzerland) in complete culture medium (CCM): Dulbecco's modified Eagle's medium (DMEM; Life Technologies, Carlsbad, CA) containing 10% fetal bovine serum (FBS; Thermo Fisher Scientific, Waltham, MA) and 1% antibiotic-antifungal preparation (100 U/ml penicillin G, 100 μg/ml streptomycin, 0.25 μg/ml amphotericin B; Antibiotic-Antimycotic; Life Technologies). Following incubation at 37 °C under 5% CO_2 for 7 days, the cells adhering to the bottom of the dish were washed with PBS and cultured in CCM. The medium was changed on day 7 at passage 0. At day 10, the cells were harvested with 0.25% trypsin and 1 mM EDTA (Trypsin-EDTA; Life Technologies) diluted by adding five volumes of PBS and centrifuged. After decanting the supernatant, the pellet was rinsed with CCM, and the cells were replated at 5×10^5 cells per 150-cm^2 dish and cultured for 6 days. The medium was changed every 3 days for 6 days during passage 1. This serial process of passaging was repeated until the cells were required for analysis and construct creation. The cells were used for creating the constructs at passage 4. Immunological surface markers and multipotency of the cells were analyzed at passage 5.

Genetic and molecular specificity of AT-MSCs

Ten thousand cells were used to analyze the specific gene expressions in MSCs. Total RNA from the cells was prepared with an RNA isolation kit (MirVana miRNA Isolation Kit; Life Technologies), according to the manufacturer's instructions. The isolated RNA was converted to cDNA and amplified with a TAKARA RT-PCR system (PCR Thermal Cycler MP; Takara Bio, Otsu, Japan) and RT-PCR kit (ReverTra Dash; Toyobo, Osaka, Japan). Specific PCR primers were used to amplify octamer-binding transcription factor 4 (OCT-4), sex-determining region Y box 2 (SOX-2), Krüppel-like factor 4 (KLF-4), cellular myelocytomatosis oncogene (C-MYC), and homeobox protein NANOG (NANOG) as premature marker genes. The conditions and expected sizes of the products are summarized in Table 1. Ten thousand cells were resuspended in 500 μl of staining buffer (SB; PBS containing 1% FBS) and incubated for

Table 1 List of PCR primers

Marker	Gene	Sequence (forward/reverse)	Ann. temp. (°C)	Fragment (bp)
Premature	OCT-4	5′-GTCGCCAGAAGGGCAAAC-3′	57.0	157
		5′-CAGGGTGGTGAAGTGAGGG-3′		
	SOX-2	5′-CCCTGCAGTACAACTCCATGAC-3′	59.0	85
		5′-GGTGCCCTGCTGCGAGTA-3′		
	KLF-4	5′-CGGCAAAACCTACACGAAGAGT-3′	59.0	119
		5′-AGTTCATCTGAGCGGGCAAAT-3′		
	NANOG	5′-CTTATTCAGGACAGCCCTGATTCTTC-3′	59.0	613
		5′-AAGACGGCCTCCAAATCACTG-3′		
	C-MYC	5′-GGATTCCGCCTCGTT-3′	55.1	184
		5′-TCTCCAAGCATCACTCG-3′		
Osteogenic	ALP	5′-ATGAGCTCAACCGGAACAA-3′	56.0	131
		5′-GTGCCCATGGTCAATCCT-3′		
	OC	5′-TCAACCCCGACTGCGACGAG-3′	68.0	204
		5′-TTGGAGCAGCTGGGATGATGG-3′		
	ON	5′-TCCGGATCTTTCCTTTGCTTTCTA-3′	57.5	187
		5′-CCTTCACATCGTGGCAAGAGTTTG-3′		
Chondrogenic	SOX-9	5′-CCGGTGCGCGTCAAC-3′	57.5	119
		5′-TGCAGGTGCGGGTACTGAT-3′		
	AGG	5′-TTCCCTGAGGCCGAGAAC-3′	65.5	194
		5′-GGGCGGTAATGGAACACAAC-3′		
Adipogenic	PPAR-γ2	5′-GCGCCCTGGCAAAGCACT-3′	59.8	238
		5′-TCCACGGAGCGAAACTGACAC-3′		
	AP2	5′-GGCCAAACCCAACCTGA-3′	59.8	167
		5′-GGGCGCCTCCATCTAAG-3′		
Housekeeping	GAPDH	5′-ACCACAGTCCATGCCATCAC-3′	60.0	450
		5′-TCCACCACCCTGTTGCTGTA-3′		

OCT-4 octamer-binding transcription factor 4, *SOX-2* sex-determining region Y box 2; *KLF-4* Krüppel-like factor 4, *NANOG*, homeobox protein NANOG, *C-MYC*, cellular myelocytomatosis oncogene, *ALP* alkaline phosphatase, *OC* osteocalcin, *ON* osteonectin, *SOX-9* sex-determining region Y-box 9, *AGG* aggrecan, *PPAR-γ2* peroxisome proliferator-activated receptor γ2, *AP2* adipocyte fatty acid-binding protein 2, *GAPDH* glyceraldehyde-3-phosphate dehydrogenase.

30 min at 4 °C with 20 μg/ml FITC-conjugated antibodies against CD34 (BD), CD45 (BD), CD90 (BD), or CD105 (Abcam, Cambridge, UK). Non-specific FITC-conjugated mouse immunoglobulin G1κ (BD) was used as a negative control. The characteristics of the antibodies are listed in Table 2. The FITC-labeled cells were washed with SB and resuspended in 500 μl of SB for fluorescence-activated cell sorting (FACS) analysis. Cell fluorescence was evaluated as a strong shift in the mean fluorescence intensity (MFI) on flow cytometry using a FACSAria II instrument (BD). The data were analyzed using FACSDiva software (BD).

Tri-lineage analysis

To investigate osteogenic differentiation, the AT-MSCs were placed in six-well plates (6 Well Plate-N; Nest Biotech, Wuxi, China) in CCM at an initial density of 5,000 cells/cm^2. After 24 h of incubation, the medium was replaced with osteogenic induction medium (Differentiation Basal Medium—Osteogenic; Lonza, Walkersville, MD), supplemented with 100 μM ascorbic acid, 10 mM β-glycerophosphate, and 1 μM dexamethasone, for 2 weeks. To investigate chondrogenic differentiation, AT-MSCs (5×10^5) were resuspended in a 15-ml culture tube (SuperClear centrifuge tubes; Labcon, Petaluma, CA) in 500 μl of chondrogenic induction medium (Differentiation Basal Medium—Chondrogenic, Lonza), supplemented with 4.5 g/l D-glucose, 350 μM L-proline, 100 nM dexamethasone, and 0.02 g/l transforming growth factor beta 3. Chondrogenic differentiation was induced in pellet cultures for 2 weeks. Adipogenic differentiation began when AT-MSCs reached a density of 5,000 cells/cm^2 in six-well plates in CCM. Following a 24-h preincubation, the medium was replaced with Adipogenic Induction Medium (Lonza), supplemented with 4.5 g/l D-glucose, 100 μM indomethacin, 10 μg/ml insulin, 0.5 mM 3-isobutyl-1-methylxanthine, and 1 μM dexamethasone, for 3 days for induction of specific genes and molecules.

The PCR primers and conditions, and the expected sizes of the products are summarized in Table 1. The osteogenic marker genes were osteocalcin (OC), osteonectin (ON), and alkaline phosphatase (ALP). The chondrogenic marker genes were sex-determining region Y-box 9 (SOX-9) and aggrecan (AGG). The adipogenic marker genes were adipocyte fatty acid-binding protein 2 (AP2) and peroxisome proliferator-activated receptor γ2 (PPAR-γ2). The reaction products were electrophoresed in a 2% agarose gel (Agarose XP; Wako Pure Chemical Industries, Osaka, Japan), and the expressions of the specific genes were determined based on the expected sizes of the bands labeled with SYBR Green (Takara Bio).

Production of calcium apatite crystals in the osteogenic extracellular matrix was evaluated with alizarin red staining in the wells of culture plates. The chondrogenic cell pellets were fixed with 10% neutral buffered formalin (NBF), embedded in paraffin, and cut into 5-μm sections using a microsection instrument. The sections were stained with alcian blue to detect cartilage-specific proteoglycans. Adipocyte-specific intracellular lipids were stained with oil red O.

Table 2 List of antibodies

Antibody	Company	Clone	Epitope	Dilution
CD34	BD	581	O-glycosylated transmembrane glycoprotein	1:5
CD45	BD	2D1	T200 family	1:2.5
CD90	BD	5E10	N-glycosylated GPI-linked membrane glycoprotein	1:10
CD105	Abcam	MEM229	Disulfide-linked glycoprotein homodimer	1:20
Isotype	BD	MOPC-21	(Not confirmed)	1:10

Preparation and implantation of 3D constructs of AT-MSCs

At least 4×10^7 AT-MSCs were used to produce each autologous construct. The cells were inoculated into eight 96-well plates (Sumitomo Bakelite, Tokyo, Japan) with 5×10^4 cells/well. After undisrupted incubation for 48 h, the cells formed spheroids with a diameter of about 700 μm in the bottom of the wells. About 760 spheroids were placed in a cylindrical mold and incubated in CCM until implantation (7 days). When the mold was carefully removed, a columnar construct of 4 mm in diameter and 6 mm in height appeared and was used for autologous implantation (Figure 1A). The general outline of this method of construction has already been reported [21,33].

The implant surgery was performed under general anesthesia using oxygen and isoflurane inhalation following premedication with sedatives and analgesics. Both femoropatellar joints were incised from the outside, and the femoral trochlear groove was exposed. Using a surgical trephine with an outer diameter of 4 mm, the articular cartilage and subchondral bone were drilled to a depth of 6 mm at the center of the groove. After removing a column of cartilage and bone, a cylindrical osteochondral defect was created in each groove (Figure 1B). A columnar construct (4 mm in diameter and 6 mm in height) composed of spheroids of AT-MSCs was autografted into the osteochondral defect in the right hind limb (Figure 1C), while no graft was implanted into the defect in the left limb (control defect, Figure 1B).

Assessment of osteochondral defects

Postoperatively, the implants and osteochondral defects were followed up every month for 6 months in animal no. 1 and 12 months in animal no. 2 using computed tomography (CT) scans of both stifles. For assessment, longitudinal section images were obtained at the maximum

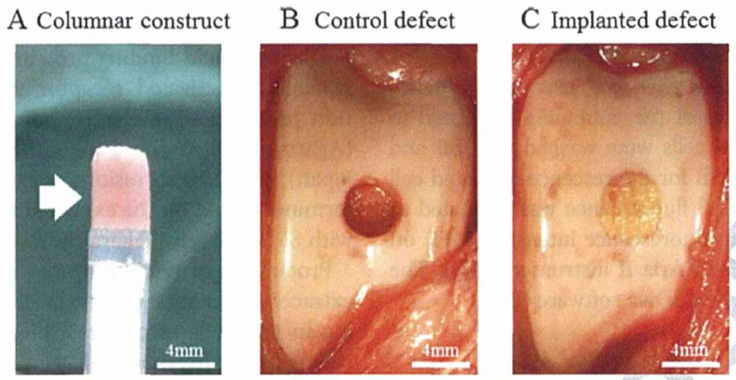

Figure 1 Surgical procedure. A columnar construct (4 mm in diameter and 6 mm in height) for the implantation **(A)**. A cylindrical osteochondral defect in each groove before implantation **(B)**. The construct composed of about 760 spheroids of AT-MSCs was autografted into the osteochondral defect in the right hind limb **(C)**. Nothing was implanted into the left limbs (control defects; **B**).

diameter in lateral views of the cylindrical defect and the maximum diameters of the radiolucent area in the images were evaluated at 0.5-mm intervals between 0 and 9 mm.

Animal no. 1 was euthanized at 6 months after surgery, and animal no. 2 was euthanized at 12 months after surgery. The macroscopic findings were scored with the International Cartilage Repair Society (ICRS) gross grading scale (Table 3). Both distal femurs were fixed in 10% NBF for 1 week and then longitudinally sectioned parallel to the trochlear groove. The tissue was decalcified with formic acid for 1 week and embedded in paraffin. Serial sections (3-μm thickness) were placed on glass slides and evaluated by Masson's trichrome staining, alcian blue staining, and immunohistochemistry using specific antibodies against collagen type II (Col-II; 1:100 dilution; Daiichi Fine Chemicals, Takaoka, Japan) and an

Table 3 ICRS gross grading scale

Feature		Score	Animal no. 1		Animal no. 2	
			Control site	Implanted site	Control site	Implanted site
Coverage	>75% fill	4	2	3	4	4
	50%–75% fill	3				
	25%–50% fill	2				
	<25% full	1				
	No fill	0				
Neocartilage color	Normal	4	1	2	3	4
	25% yellow/brown	3				
	50% yellow/brown	2				
	75% yellow/brown	1				
	100% yellow/brown	0				
Defect margins	Invisible	4	1	2	3	3
	25% circumference visible	3				
	50% circumference visible	2				
	75% circumference visible	1				
	Entire circumference visible	0				
Surface	Smooth/level with normal	4	0	2	3	3
	Smooth but raised	3				
	Irregular 25%–50%	2				
	Irregular 50%–75%	1				
	Irregular >75%	0				
Average (0–4)			1.0	2.25	3.25	3.5

Avidin-Biotin Enzyme Complex system (VECTASTAIN ABC Standard Kit; Vector Laboratories, Southfield, MI). The histopathologic findings were scored with the ICRS histological grading scale (Table 4).

Results

Genetic and molecular characteristics and tri-lineage potential of AT-MSCs

Porcine AT-MSCs adhering to the bottom of the culture dish were spindle-shaped and proliferated well (Figure 2A), reaching over 1×10^6 and 1×10^7 cells at passage 3 and passage 4, respectively. A strong shift in MFI on flow cytometry was detected with antibodies against CD90 and CD105 (Figure 3A, B), while no signals were detected with antibodies against CD34 and CD45 (Figure 3C, D). The genetic markers of OCT-4, SOX-2, KLF-4, C-MYC, and NANOG were all positive (Figure 4A). Following osteogenic induction, AT-MSCs aggregated and contracted to form colonies (Figure 2B), and expressions of specific marker genes, including ALP, OC, and ON, were detected (Figure 4B). These cells also showed appropriate characteristics of the stroma, including staining with alizarin red, indicating the presence of calcium apatite crystals (Figure 2B). Reverse transcription PCR (RT-PCR) of AT-MSCs placed in chondrogenic induction medium revealed the expressions of marker genes, including SOX-9 and AGG (Figure 4B). Histological observation of the cell pellets showed a hyaline cartilage-like structure that was positively stained with alcian blue (Figure 2C). Adipogenic induction of the AT-MSCs resulted in adipocyte-like flattened cells with small lipid vesicles that were positively stained with oil red O (Figure 2D). RT-PCR revealed significant increases in adipogenic marker gene expressions such as AP2 and PPAR-γ2 (Figure 4B).

CT images

The reduction in the subchondral radiolucent area of the implanted site became more dramatic at 2 or 3 months after surgery compared with the control site in the both animals (Figure 5). CT images at 6 months after surgery for animal no. 1 are shown in Figure 5A. A radiopaque area emerged from the boundary between the bone and the implant and increased more steadily upward and inward for the implanted defect (the right femur) as time passed after surgery, compared with the control site. The radiolucent area of the implant diminished in a stepwise manner and then degraded to a diameter of 1 mm by 5 months after surgery. CT images at 12 months after surgery for animal no. 2 are shown in Figure 5B. A radiopaque area of the implant emerged in the same manner as in animal no. 1, gradually progressed, and then filled the entire osteochondral defect

Table 4 ICRS histological grading scale

Feature		Score	Animal no. 1		Animal no. 2	
			Control site	Implanted site	Control site	Implanted site
Surface	Smooth/continuous	3	0	3	3	3
	Discontinuities/irregularity	0				
Matrix	Hyaline	3	0	1	1	2
	Mixture; hyaline/fibrocartilage	2				
	Fibrocartilage	1				
	Fibrous tissue	0				
Cell distribution	Columnar	3	0	0	0	2
	Mixed/columnar clusters	2				
	Clusters	1				
	Individual cells/disorganized	0				
Viability of cell population	Predominantly viable	3	3	3	3	3
	Partially viable	1				
	<10% viable	0				
Subchondral bone	Normal	3	1	2	0	2
	Increased remodeling	2				
	Bone necrosis/granulation tissue	1				
	Detached/fracture/callus at base	0				
Cartilage mineralization (calcified cartilage)	Normal	3	0	3	3	3
	Abnormal/inappropriate location	0				
Average (0–3)			0.67	2	1.67	2.5